Interpretation of data in multidimensional spaces and its application to Coulomb-explosion imaging

Jacob Levin, Dror Kella, and Zeev Vager
Department of Particle Physics, Weizmann Institute, Rehovot, Israel
(Received 12 September 1995)

A solution is presented for the problem of interpreting measurements of data from many degrees of freedom where binning is prohibitive. A binninglike procedure is introduced in which data and theory are represented by a set of independent expectation values. A comparison between theory and experiment is then performed by a conventional procedure together with an additional test of the independence of the expectation values. Associated uncorrelated errors are derived as well. The application of this method to Coulomb-explosion imaging is discussed. The method is illustrated by the analysis of the bending angle distribution of the CH_2^+ molecule from Coulomb-explosion imaging measurements.

PACS number(s): 33.15.−e, 34.10.+x

I. INTRODUCTION

This paper deals with the methodology of comparing experimental values to a model or theory. For data sets with few degrees of freedom the subject is so well digested that every aspect of it seems to be already documented [1–3, and references therein]. Yet, we find a lack of proper treatment when dealing with data comprising a list of events that were measured in a multidimensional space. An optimal method of comparing the experimental values to the theory is missing. We hope that this paper will fill the gap.

The motivation for writing this paper is to formulate a methodical analysis of the data of Coulomb-explosion imaging (CEI). The subject of CEI will be introduced in the next section. The method of analysis is general enough that the reader who might be uninterested in CEI can skip that section without losing insight.

The conventional method of comparing experimentally measured events to theory is first to divide the space of the measured values into discrete cells, commonly called bins. The histogram, which is the distribution of the events in the bins, establishes the grounds for comparing independent probabilities of measured events to the theory. For instance, in the χ^2 test [1,2] a comparison is made between the number of bins and the sum over the bins of squares of error-normalized differences between data and theory. In many experiments, the estimation of the theoretical probability within a given bin is indirect, namely, a Monte Carlo simulation of the experiment is performed and a simulated histogram is collected. A well-defined comparison can be made only if the statistics of the simulated data is large enough to allow an estimate of ''theoretical'' errors in each bin.

In general, such a procedure is prohibitive for events that are measured in a multidimensional space of coordinates (unless the distribution is separable within that space). First, the multidimensional histogram is not useful because of its immense number of bins within any reasonably chosen bin size. Second, the table of coordinates of measured events cannot be directly compared with the table of coordinates of simulated events without specifying a common bin in space for each comparison. Interpolation methods have been devised to overcome these problems with a disadvantage of losing the independence of the content of each bin [4,5]. We have encountered such problems in the analysis of CEI data (see the next section) and present in this paper a general solution to the problem.

The essence of the solution is to replace the conventional binning by a minimal bins representation (MBINS), which is a set of expectation values of carefully chosen orthonormal functions of the measured coordinates. Those functions can be chosen such that the MBINS are statistically independent and therefore the collection of MBINS replaces the histogram, and a comparison with theory is simply performed as in the conventional methodology. As a result the error processing, taking into account correlations, is carried out by simple and transparent means.

II. CEI MEASUREMENTS

CEI [5–7] is a relatively new method for direct determination of molecular structure, as well as the correlated density of nuclei within the molecule. It provides a set of experimental values associated with all the nuclear coordinates of each individually measured molecule. When a substantial number of molecules is collected one obtains a sample representing the nuclear distribution function of the measured ensemble. The general method presented in this paper is used for retrieving this distribution from the raw data accompanied by a reliable error estimate. The CEI method for arriving at the correlated nuclear distribution function is unique in the sense that it directly extracts such distributions from the data without using, possibly biased, *a priori* theoretical assumptions (e.g., adiabatic approximations). Therefore, the rigorous procedure of extraction of information from the data and the precise definition of errors is of importance. An illustrative one-dimensional example is given in Sec. VI, where the bending motion of CH_2^+ is analyzed.

A full description of the CEI method and the experimental setup can be found in several previous publications [7–11]. For completeness we will outline the principle of the method. Accelerated molecules are stripped of their binding electrons in an extremely thin foil. The stripping process is fast enough to justify the employment of the sudden approxi-

mation of switching between the molecular Hamiltonian to an almost pure Coulomb Hamiltonian of the residual atomic ion fragments. The Coulomb repulsion separates the ion fragments, and the asymptotic velocities of all the molecular fragments are measured, one molecule at a time. Such an event is recorded in a $3M$ dimensional space, where M is the number of atoms in the molecule. This space is closely related to the asymptotic velocity coordinate space created by the final-state interaction of pure Coulomb repulsion between the measured ion fragments. It will be referred to here as the V space.

The problem of extracting the optimal nuclear density function in configuration space (R space) from the measured ensemble of events has been mentioned in previous publications of CEI [12]. A Monte Carlo simulation of the Coulomb trajectories has been developed that takes into account the interaction of the molecules with the target [13]. When separable V and R spaces are assumed, the problem reduces to finding the optimal set of one-dimensional densities. These are treated by conventional methods of least-squares fit, which include binning into histograms. As was mentioned above, such methods are not suitable for nonseparable multidimensional conversion problems where proper binning is prohibitive. Previous attempts to overcome the general multidimensional conversion problem were partially successful [4] but the complete solution became possible only by further developments, which are described below.

III. MINIMAL REPRESENTATION

Assume that a table of measured events in a multidimensional space is given. The boundary of this space, outside of which no data exist, could be simply determined. Imagine a complete set of orthonormal functions that are defined in this space. The physical nature of the data limits the complexity of the relevant functions; for example, if the data contain events from an angular correlation of a cascade, then the possible multipolarities and the involved spins limit the variety of functions to a relatively small finite number. In CEI, the number of nodes in the relevant functions is limited by the finite kinetic energy of the measured species. These restrictions on the orthonormal functions to be used for the description of the probability function of the measured events has to come from general physical understanding of the nature of the measured system and the measuring apparatus. As a general rule, the experimental probability distribution is assumed to be described by a linear combination of many functions, but their number is by far smaller than the number of appropriate bins in the conventional histogram treatment.

Let $\{\vec{v}_\alpha\}$ ($\alpha=1,2,\ldots,N$) be the ensemble of coordinates of N individually measured events (V space in CEI) and $f_k(\vec{v})$ are a chosen set of smooth orthonormal functions defined in this space.

Define the kth estimator $[f_k]$ by

$$[f_k]\equiv[f_k(\vec{v}_\alpha)]_\alpha\equiv\frac{1}{N}\sum_{\alpha=1}^{N} f_k(\vec{v}_\alpha) \tag{1}$$

and an expansion function

$$F(\vec{v})=\sum\,[f_k]f_k(\vec{v})=[\tilde{f}]\bar{f}(\vec{v}), \tag{2}$$

where the symbol $[\tilde{f}]$ is used for a row of coefficients $[f_k]$ and $\bar{f}(\vec{v})$ for a column of functions $f_k(\vec{v})$ (a bar symbolizes a column "matrix" and a tilde symbolizes its transpose).

Theorem: If the exact physical probability function can be expanded by the set $f_k(\vec{v})$, then $F(\vec{v})$ [given by Eq. (2)] is the optimal expansion in the sense that it approaches the exact expansion for $N\to\infty$.

(*Proof*: If $G(\vec{v})$ is the exact physical probability function, then the theorem supposes

$$G(\vec{v})=\sum\,G_k f_k(\vec{v}),$$

where

$$G_k=\int f_k(\vec{v})G(\vec{v})d\vec{v}.$$

But $\vec{v}_\alpha$ is a sample of the exact probability function $G(\vec{v})$, thus by the central limit theorem

$$\lim_{N\to\infty}\frac{1}{N}\sum_{\alpha=1}^{N} f_k(\vec{v}_\alpha)=\int f_k(\vec{v})G(\vec{v})d\vec{v}$$

and $[f_k]\to G_k$ as N increases [1].)

This approach accommodates itself to any number of dimensions without the need for defining multidimensional bin size, cuts, projections, or histograms. This is especially important in multidimensional problems where choosing a fine resolution bin size is in conflict with having good statistics within the bin.

The covariance matrix elements describing the average correlation of deviations of the coefficients $[f_k]$ are

$$\mathrm{cov}(k,\hat{k})=[\{f_k(\vec{v}_\alpha)-[f_k]\}\{f_{\hat{k}}(\vec{v}_\alpha)-[f_{\hat{k}}]\}]_\alpha, \tag{3}$$

thus, the theoretical error matrix elements of the $[f_k]$ experimental estimators are

$$E_r(k,\hat{k})=\mathrm{cov}(k,\hat{k})/(N-P), \tag{4}$$

where P is the number of coefficients that are used to describe the estimated probability function of the data. A relatively small set of coefficients $[f_k]$ portrays the "spectrum" of the data in the f_k representation, but, unlike histograms, there must still be correlations that are manifested by the nondiagonal terms of E_r. This can be rectified by an orthonormal transformation, T, which diagonalizes E_r and transforms the functions $\bar{f}(\vec{v})$ and the coefficients $[\bar{f}]$ into a new set of orthonormal expansion functions and coefficients

$$\bar{s}(\vec{v})=T\bar{f}(\vec{v}),\quad [s]=T[f]. \tag{5}$$

The uncorrelated errors are given by

$$TE_r\tilde{T}=\sigma^2, \tag{6}$$

where σ^2 is a diagonal matrix of positive elements.

We have reached an estimated probability function given by a vector of parameters $[s_1],\ldots,[s_P]$ and associated errors $\sigma_1,\ldots,\sigma_P$ which are statistically equivalent to the measured ensemble $\{v_\alpha\}$. The multidimensional coordinates list of events are now represented by MBINS and associated errors.

IV. EXPERIMENTAL VERIFICATION OF A PARAMETERLESS THEORY

Assume that a well-planned experiment is designed to test such a theory. If the theory is correct, then the results of the measurement are predictable within the experimentally imposed accuracy. The verification is performed by negation: if the simulation is inconsistent with the results of the measurement, then the theory (or the experiment) is rejected within some statistical confidence level. Thus, initially, the theory is assumed to be correct. Normally, it is easier to collect simulated data than experimental data. Therefore, a better picture of the minimal representation is obtained by using a large simulated sample $\{\vec{v}_\beta^{(s)}\}$ $(\beta=1,2,\ldots,N^{(s)})$ and following the procedure outlined in the preceding section to obtain the MBINS representation of the data as predicted by the theory.

The experimental error matrix, defined by N events, can be derived from the simulation as follows. The simulated covariance matrix elements are

$$\mathrm{cov}^{(s)}(k,\hat{k})=[\{f_k^{(s)}(\vec{v}_\beta^{(s)})-[f_k^{(s)}]\}\{f_{\hat{k}}^{(s)}(\vec{v}_\beta^{(s)})-[f_{\hat{k}}^{(s)}]\}]_\beta. \tag{7}$$

Thus, the estimate for the experimental error matrix is

$$E_r^{(s)}(k,\hat{k})=\mathrm{cov}^{(s)}(k,\hat{k})/(N-P). \tag{8}$$

This matrix depends on the number of experimental events N rather than $N^{(s)}$.

This can be employed by the experimentalist for a judgment of the finesse of the test of the theory by the given statistics of the measurements in the following way. The (N dependent) sensitivity of the measurement of $[s_k]$ is estimated by

$$[S_k^{(s)}]=\frac{[s_k^{(s)}]}{\sigma_k^{(s)}}. \tag{9}$$

If $[S_k^{(s)}]<1$, then the measurement is insensitive to the function $s_k^{(s)}(\vec{v})$. This suggests a congruent transformation to the coefficients $[\bar{s}^{(s)}]$ and the functions $\bar{s}^{(s)}(\vec{v})$ as follows:

$$[\bar{S}^{(s)}]=\sigma^{(s)-1}[\bar{s}^{(s)}],\quad \bar{S}^{(s)}(\vec{v})=\sigma^{(s)}\bar{s}^{(s)}(\vec{v}). \tag{10}$$

In the spirit of the verification by negation we have selected only the theoretically meaningful set of functions $s_1^{(s)}(\vec{v}),\ldots,s_P^{(s)}(\vec{v})$. Now, we further reduce the set to indices for which $[S_k^{(s)}]>1$ because of the finite statistics of the experiment. We also rename the indices to be from 1 to $\mathscr{P}\leqslant P$. The estimated error matrix in this minimal representation of orthogonal functions $\bar{S}^{(s)}$ is a unit matrix with rank $\mathscr{P}$. We expect that looking at the data with this MBINS of the functions $\bar{S}^{(s)}$ should statistically reproduce the unit error matrix and the expectation values $[\bar{S}^{(s)}]$ (all above 1 and with a unit standard deviation) for a theory that is consistent with the measurement.

This test is accomplished by the evaluation of a new matrix:

$$\Psi(k,\hat{k})=[\{S_k^{(s)}(\vec{v}_\alpha)-[S_k^{(s)}]\}\{S_{\hat{k}}^{(s)}(\vec{v}_\alpha)-[S_{\hat{k}}^{(s)}]\}]_\alpha. \tag{11}$$

Notice that the above Ψ test elements are evaluated by using ensemble averages of the measured data. The similarity to a χ^2 test is quite clear. The $[S_k^{(s)}]$ are theoretical expectations with a unit standard deviation and therefore the diagonal elements are the conventional normalized χ^2 tests. The appreciation of the confidence level of the theory of such distributions are well documented. There is an additional requirement that the absolute value of the off-diagonal elements of Ψ are much smaller than 1 which, if reached, assures that the MBINS are independent of each other.

This Ψ test is not limited to the restricted MBINS functions but can be extended to more functions from the complete set $\bar{S}^{(s)}$ with either theoretical or statistical expectation values that are equal to zero. Of course, such an extension would comprise a more stringent test of the theory and can be useful for finding features of the experimental data that are not explained by the theory. An obvious case like this occurs when the MBINS defined by the measured data (Sec. III) contain more significant expectation values than the MBINS defined by the theoretically simulated data.

To summarize, $\mathscr{P}$ independent χ^2 tests are suggested for examining the consistency of the theory with the measured array of events without the need of binning or histograms. A check of the independence of those tests is suggested as well.

V. THEORY WITH ADJUSTABLE PARAMETERS

We consider two types of parameter dependence of theories: linear and nonlinear. We start with the linearly-dependent theories and later generalize to cases where linear iterations are converging.

Most of the measurements in physics are indirect in the sense that the space where the experimental values are recorded through the experimental apparatus is not the space where the fundamental physics occurs. For example: the structure of molecules is measured by spectroscopic measurements of electromagnetic radiation; or the interaction of nuclear multipoles with lattice fields may be measured by the angular correlation of different radiations.

Call R space the space of the interesting physics (for CEI this is the configuration space of the molecules under study) and assume that the theory of the underlying physics can be expressed as a density function in this space, which is given by a linear combination of orthonormal functions. Let $\mathscr{G}(\vec{r})$ be an initial guess for the R-space density

$$\mathscr{G}(\vec{r})=\sum\ [g_q]g_q(\vec{r})=[\tilde{g}]\bar{g}(\vec{r}), \tag{12}$$

where $g_q(\vec{r})$ are a set of assumed orthonormal functions with assumed coefficients $[g_q]$.

Given $\mathscr{G}(\vec{r})$, events in R space can be simulated. Assuming that $[\bar{g}]$ are the correct coefficients then the MBINS are realized by the $\bar{S}^{(s)}(\vec{v})$ functions and $[\bar{S}^{(s)}]$ coefficients. The direction of simulation calculations is always from $[\bar{g}]$ to $[\bar{S}^{(s)}]$. Symbolically

$$[g] \Rightarrow \text{simulations} \Rightarrow [\bar{S}^{(s)}]. \tag{13}$$

Finally, the vector $[\bar{S}]$ is calculated from the experimental data with the aid of the $\bar{S}^{(s)}(\vec{v})$ representation, and we define a difference vector,

$$\delta[\bar{S}] = [\bar{S}] - [\bar{S}^{(s)}]. \tag{14}$$

If indeed the coefficients $[g_q]$ are optimal, then $\delta[\bar{S}]$ elements approach zero such that their absolute value is less than the unit standard deviation. If this is not the case, then the aim is to minimize this difference by changing the initial linear combination in R space, namely, by changing $[\bar{g}]$. This should be done in a least-squares fashion, remembering that the statistical weight of the components of $\delta[\bar{S}_k]$ are the same. It can be performed uniquely only if the number of parameters is smaller than or equal to $\mathscr{P}$ — the number of components of $[\bar{S}^{(s)}]$. For simplicity and without loosing generality we start by choosing $\mathscr{P}$ parameters in the R-space representation.

A linearized matrix K connecting $\delta[\bar{S}]$ to a correction $\delta[\bar{g}]$ can be calculated by varying the parameters $[\bar{g}]$ one at a time and recalculating simulated events, keeping the representation $\bar{S}^{(s)}(\vec{v})$ intact:

$$\delta[\bar{S}] = K\delta[\bar{g}]. \tag{15}$$

The remaining task for the next iteration is to ''invert'' K in Eq. (15). This will enable the evaluation of the correction $\delta[\bar{g}]$ as well as the transformation of the error matrix from V space to R space as required. For truly linear $\mathscr{G}(\vec{r})$ there are no further iterations and this step gives the optimal $\delta[\bar{g}]$ in the least-squares sense. This task belongs to the general methodology of the linear extraction of measured parameter values from data. The analysis below closely follows the methods developed by Monahan [3].

The symmetric matrices $K\tilde{K}$ and $\tilde{K}K$ have common and positive eigenvalues $\Lambda_1^2, \ldots, \Lambda_{\mathscr{P}}^2$,

$$\tilde{V}K\tilde{K}V = \tilde{R}\tilde{K}KR = \Lambda^2, \tag{16}$$

where Λ^2 is a diagonal matrix. Yet, the diagonalizing matrices, V and R respectively, are not only different, but are built from eigenvectors out of the spaces $\delta[\bar{S}]$ and $\delta[\bar{g}]$, respectively (notice that K has meaningful left operations on the V-space vector $\delta[\bar{S}]$ and meaningful right operations on the R-space vector $\delta[\bar{g}]$). The sign of the eigenvectors in R and V can be chosen such that

$$KR = V\Lambda, \tag{17}$$

where Λ is the positive square root of Λ^2.

With this choice of V and R the ordinary inverse of K can be expressed as

$$K^{-1} = R\Lambda^{-1}\tilde{V}. \tag{18}$$

When K^{-1} is used to solve Eq. (15) then very small Λ_i amplify small components in V space, which are parallel to V_i, into large components in R space, which are parallel to R_i. The significance of such components can be evaluated by propagating the unit error matrix of the $\bar{S}^{(s)}(\vec{v})$ representation (the orthogonal transformation V does not alter the unit matrix) into an R-space representation. Specifically, the $\bar{G}(\vec{r}) = \tilde{R}\bar{g}(\vec{r})$ orthonormal representation has the Λ^{-2} diagonal error matrix and $[\bar{G}] = \tilde{R}[\bar{g}]$ expansion coefficients. The nature of the experimental apparatus and the final statistics do not allow an accurate determination of parameters when $[G_k] < \Lambda_k^{-1}$. Thus, the expansion in R space is reduced to $\mathscr{Q}$ functions in which the expansion coefficients are significantly different from zero, i.e., $[G_k] > \Lambda_k^{-1}$. The iteration procedure is stopped when all the linear corrections to the significant parameters are within the one standard deviation limit, namely, $\delta[G_q] < \Lambda_q^{-1}$. Finally the R-space distribution is represented by $\mathscr{Q}$ orthogonal functions $G_q(\vec{r})$ as

$$\mathscr{G}(\vec{r}) = \sum_{q=1}^{\mathscr{Q}} [G_q] G_q(\vec{r}) \tag{19}$$

with the corresponding independent errors for the coefficients $[\bar{G}]$,

$$\Lambda_1^{-1}, \ldots, \Lambda_{\mathscr{Q}}^{-1}. \tag{20}$$

As was mentioned above, we expect the number $\mathscr{Q}$ of final significant parameters in R space to be less or equal to the number of the significant parameters $\mathscr{P}$ of the data in V space. The final test of the results is performed by a direct comparison of the data to the simulated distribution in V space by the Ψ test, as described in Sec. III, Eq. (11).

VI. ILLUSTRATIVE EXAMPLE

A one-dimensional example is outlined here in order to illustrate the analysis procedure. This enables the illustration of different features by the aid of graphs and histograms which is difficult in the multidimensional cases.

A. CEI of cold CH_2^+

The CEI measurement of the CH_2^+ molecule has been reported earlier and the reader is referred to Ref. [12] for a detailed description of the experimental setup and the results. A short review is given below and is followed by a one-dimensional analysis of the bending mode of a vibrationally cold CH_2^+. It is given as a simple and easily visualized example of the general method presented above.

Cold CH_2^+ ions were accelerated to 3.9 MeV by the 5MV Dynamitron at Argonne National Laboratory. The fast ions entered a scattering chamber where they were stripped of their valence electrons by a 0.6 μg/cm^2 Formvar target. This fast stripping (less than 10^{-16} sec) initiated an energetic Coulomb repulsion between the atomic fragment ions. The ions emerging from the target were directed towards position- and time-sensitive detectors. From the position (x,y) and time (z) coordinates provided by these detectors,

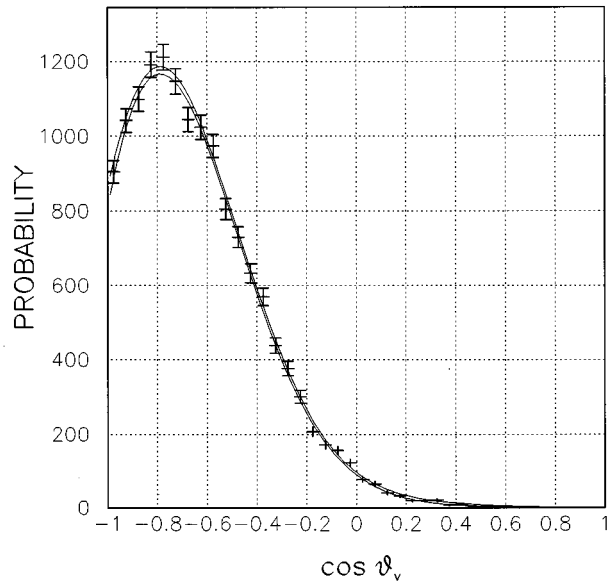

FIG. 1. Angular distribution of the CH_2^+ molecule in V space is represented by (a) the conventional histogram representation and (b) a smooth function given by a combination of four orthogonal functions with coefficients and errors listed in Table I. The function is plotted within error limits.

masses, charge states, and final velocities were extracted for each fragment, thus yielding a nine-component vector describing each molecule in the beam. The velocity vectors $\vec{v}_1$ and $\vec{v}_2$ of the two protons that were measured relative to the carbon were extracted and a "V-space bond angle" θ_v was defined as the angle between these two velocity vectors.

This V-space angle θ_v is closely related to the more familiar internal coordinate bond angle θ_r (see Ref. [12]). Since the bending of CH_2^+ was found to be uncorrelated to the other modes of internal motion it could be treated separately as a one-dimensional problem. The distribution of $\cos(\theta_v)$ is shown in Fig. 1 in a histogram form with statistical errors. This is the raw data where target effects (such as multiple scattering and charge exchange) that cause smearing of the data are present. It is important to reemphasize that

TABLE I. Uncorrelated-error representation of V-space data with $P=4$.

n	$[s]_n$	σ_n	$[s]_n/\sigma_n$
1	0.912	0.000 508	1795
2	0.527	0.003 95	133.5
3	-0.348	0.008 24	-42.3
4	0.015 8	0.009 51	1.7

such convenience of a histogram and display of statistical errors of data stored in bins is not practicable for multidimensional problems.

B. Characterization of the CEI data

A Gaussian fit to the histogram of Fig. 1 suggested the use of Gaussian weighted functions of the form

$$f_n(x_v)=P_n(x_v)\exp\left(\frac{(x_v-x_v^0)^2}{2\sigma_v^2}\right), \tag{21}$$

where $x_v=\cos\theta_v$. The choice $x_v^0=-1$ was made for illustrative purposes and σ_v was derived directly from the data. The polynomials $P_n(x_v)$ were derived by a Graham-Schmidt orthogonalization of the set $\{1,x,x^2,\ldots,x^n\}$, such that [14]

$$\int_{-1}^{1} f_i(x_v)f_j(x_v)dx_v=\delta_{i,j}\,. \tag{22}$$

The angular distribution was expanded by a finite set of functions $f_n(x_v)$ by means of Eqs. (1) and (2). We used an expansion up to the third power in P_n (four expansion functions) and checked by inspection that additional terms did not modify the solution $F(x_v)$ within its experimental error. Of course, the last step is impossible for the multidimensional cases. We looked for the statistically significant coefficients in the uncorrelated error representation $\bar{s}(x_v)$ [Eqs. (5) and (6)]. Table I lists all the coefficients $[s_k]$ with their associated errors. The table shows that all the coefficients are significantly different from zero and their number cannot be

TABLE II. Uncorrelated-error representation of the reconstructed R space. The results of three iterations are listed. For each iteration the coefficients of the nondiagonal representation $[g]$ and parameter σ_r are quoted.

Iteration	n	$[G]_n$	$\delta[G]_n$	$\sigma_n^{[G]}$	
1	1	0.186	0.125	0.016 3	$\sigma_r=0.456$
	2	-0.194	-0.219	0.011 8	$[g]=\{1.098,0.104,-0.109,0.037\,0\}$
	3	0.664	0.128	0.005 63	
	4	-0.846	-0.002 96	0.000 514	
2	1	0.005 44	0.183	0.041 7	$\sigma_r=0.324$
	2	-0.310	0.060 4	0.019 7	$[g]=\{1.26,0.252,-0.166,0.052\,0\}$
	3	0.492	-0.070	0.012 0	
	4	-1.17	-0.003 70	0.000 927	
3	1	-0.019 5	-0.008 23	0.048 4	$\sigma_r=0.357$
	2	0.244	0.000 186	0.019 9	$[g]=\{1.24,0.167,-0.186,0.006\,7\}$
	3	-0.488	-0.000 694	0.011 6	
	4	-1.14	-0.002 55	0.001 83	

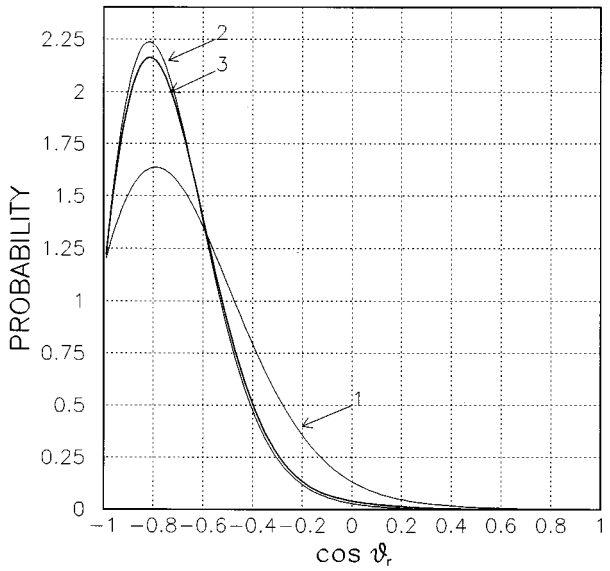

FIG. 2. Distribution of the bending angle in CH_2^+. The results of three iterations of the inversion procedure are plotted. The lines correspond to the coefficients given in Table II.

reduced, thus $\mathscr{P} = P = 4$. The result is illustrated in Fig. 1 where the corresponding distribution function $F(x_v)$ is shown within one standard deviation error limits. Note that the histogram representation is replaced by an equivalent representation that contains only four values and their uncorrelated errors.

C. Characterization of *R* space

The simple illustration above is continued here for the extraction of the measured R-space density. Following the prescription given in Sec. V, we assumed as a first guess that the R-space angles are distributed exactly as the V-space angles,

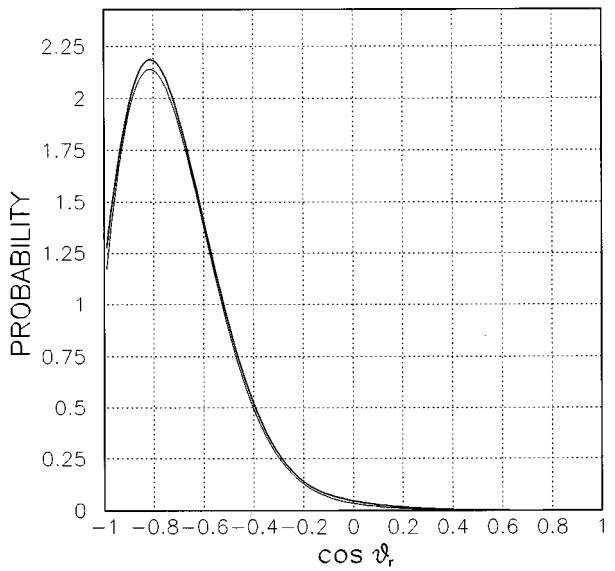

FIG. 3. Result of the third iteration in Fig. 2 is plotted again within its error limits.

TABLE III. Ψ matrix for CH_2^+ analysis.

Ψ			
0.568	-0.115	0.006 88	-0.001 58
-0.115	0.954	0.002 00	0.005 19
0.00688	0.002 00	1.013	0.004 98
-0.00158	0.005 19	0.004 98	0.995

$$g_n(x_r) = P_n(x_r)\exp\left(\frac{(x_r - x_r^0)^2}{2\sigma_r^2}\right) \tag{23}$$

with $\sigma_r = \sigma_v$, $x_r^0 = x_v^0$ and the initial coefficients $[g] = [f]$. Such an assumption is a reasonable starting point for any molecule of the form XH_n, where X is a heavy ion. In such cases the Coulomb interaction between the protons is weak in comparison with the X-H interaction, and the angles are almost unaltered during the explosion. Nevertheless, the following iterative procedure will complete the missing information and yield the needed corrections in the R-space distribution.

The linearized transformation K was calculated as in Eq. 15. By inverting K we found the corrections $\delta[G]$ and $\delta[g] = R\,\delta[G]$. The next iteration started in sampling the new R-space distribution defined by $[g] + \delta[g]$. At this point we modified the representation by calculating a new σ_r in the expansion (21). This had the advantage of both reducing the number of iterations and the number of the expansion terms.

The results of the three iterations are listed in Table II. The coefficients $[G]$, their corrections $\delta[G]$ and the uncorrelated errors $\sigma^{[G]}$ are calculated by the procedure given at the end of Sec. V. The corresponding coefficients of the functions $g_n(x_v)$ and the parameters σ_r are also given for reference. The corrections $\delta[G]$ after the third iteration are of the

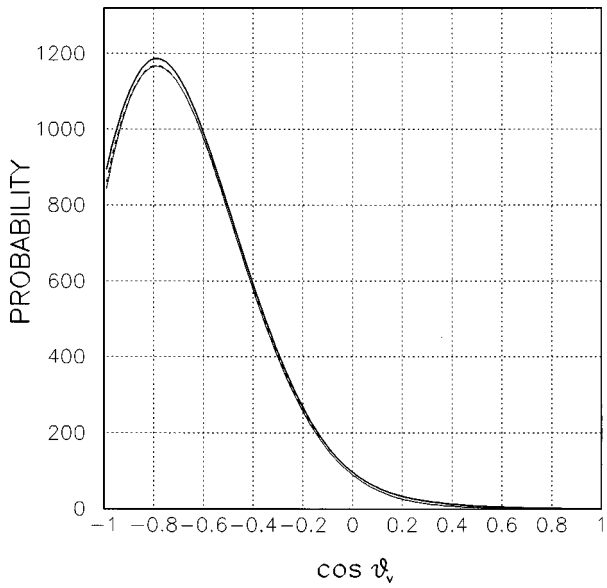

FIG. 4. Same measured angular distribution function as Fig. 1 is plotted within error limits. It is compared to the V-space distribution function that is produced by simulation from the R-space distribution in Fig. 3 (dashed line).

order of the error or smaller and the coefficient $[G]_1$ is statistically equivalent to zero. Figure 2 shows the distributions $\mathcal{G}(x_v)$ [Eq. (19)] that correspond to Table II, and Fig. 3 presents the final result within one $\sigma^{[G]}$ error limits. We used the advantage of a one-dimensional presentation to check directly that the distribution of the next iteration lies inside these limits, as could be expected from the results in Table II.

The Ψ matrix test was performed and presented in Table III. The diagonal terms are close to 1 as expected, except for the first term, which is correlated to the other terms. We suspect the calculation of K on a finite sample to be the origin of this correlation. The convergence is demonstrated directly in Fig. 4 where the simulated V-space distribution is compared to the data, showing a full agreement within the statistical error.

VII. CONCLUSION

We presented an algorithm for extracting meaningful density functions from samples in a multidimensional space. The source of the samples is not restricted to CEI data and its interpretation in terms of density functions of nuclear coordinates within molecules. The problem of an estimation of a smooth multidimensional function from calculated or measured samples is quite general in fields such as quantum chemistry, particle physics (experiment and theory), as well as plasma physics. We hope that the contents of this manuscript will contribute to the methodology of such analysis. The principle of the method is based on well known routines of data analysis and error estimates, except for the complications of dealing with multidimensional spaces, which do not allow a simple extension of the lower dimensional methods. For example, the need for binning is avoided completely. This is possible only because of previous information that molecules are defined within a bound space and that low-lying excitations of molecules require smooth density functions within this space. As a result, the density functions are described by a manageable number of parameters. Those parameters can be extracted and their accuracy and correlations can be derived. The common problem of error amplification by a nearly singular transformation Jacobian is overcome by well known statistical methods.

ACKNOWLEDGMENT

This research is supported by Minerva Foundation, Munich, Germany.

[1] R. J. Barlow, *Statistics* (Wiley, New York, 1989).
[2] S. L. Meyer, *Data Analysis for Scientists and Engineers* (Wiley, New York, 1975).
[3] J. E. Monahan, in *Scintillation Spectroscopy of Gamma Radiation*, edited by S. M. Shafroth (Gordon and Breach, New York, 1967).
[4] D. Kella and Z. Vager, J. Chem. Phys. **102**, 8424 (1995).
[5] D. Kella, Ph.D. thesis, Weizmann Institute of Science, 1994 (unpublished).
[6] T. J. Graber, Ph.D. thesis, Argonne National Laboratory, 1993 (unpublished).
[7] Z. Vager, R. Naaman, and E. P. Kanter, Science **244**, 426 (1989).
[8] D. Kella, M. Algranati, H. Feldman, O. Heber, H. Kovner, E. Malkin, E. Miklazky, R. Naaman, D. Zajfman, J. Zajfman, and Z. Vager, Nucl. Instrum. Methods **A329**, 440 (1993).
[9] T. Graber, D. Zajfman, E. P. Kanter, R. Naaman, Z. Vager, and B. J. Zabransky, Rev. Sci. Instrum. **63**, 3569 (1992).
[10] D. Zajfman, A. Belkacem, T. Graber, E. P. Kanter, R. E. Mitchell, R. Naaman, Z. Vager, and B. J. Zabransky, J. Chem. Phys. **94**, 2543 (1991).
[11] A. Belkacem, A. Faibis, E. P. Kanter, W. Koenig, R. E. Mitchell, Z. Vager, and B. J. Zabransky, Rev. Sci. Instrum. **61**, 946 (1990).
[12] T. Graber, E. P. Kanter, Z. Vager, and D. Zajfman, J. Chem. Phys. **98**, 7725 (1993).
[13] D. Zajfman, T. Graber, E. P. Kanter, and Z. Vager, Phys. Rev. A **46**, 194 (1992).
[14] G. Arfken, *Mathematical Methods for Physicists* (Academic, New York, 1985).